We are IntechOpen, the world's leading publisher of Open Access books Built by scientists, for scientists

6,900
Open access books available

185,000
International authors and editors

200M
Downloads

154
Countries delivered to

Our authors are among the

TOP 1%
most cited scientists

12.2%
Contributors from top 500 universities

CLARIVATE ANALYTICS
BOOK CITATION INDEX
INDEXED

WEB OF SCIENCE™

Selection of our books indexed in the Book Citation Index
in Web of Science™ Core Collection (BKCI)

Interested in publishing with us?
Contact book.department@intechopen.com

Numbers displayed above are based on latest data collected.
For more information visit www.intechopen.com

The Influence of the Concealed Pollution Sources Upon the Indoor Air Quality in Detached Houses

Motoya Hayashi, Yishinori Honma and Haruki Osawa

Additional information is available at the end of the chapter

http://dx.doi.org/10.5772/45767

1. Introduction

There are many infiltration routes in Japanese traditional wooden houses. The equivalent leakage areas of recent houses have become smaller but the infiltration routes are left in the concealed spaces like beam spaces, crawl spaces and inside-wall spaces. The previous studies in test houses showed that these routes lead chemical compounds into the indoor spaces from the concealed spaces as in [1]. Therefore, the infiltration from concealed spaces was taken into consideration in the amendment of Japanese building standard law in 2003 as in [2], [3].

Common Japanese houses are composed of post-and-beam structures and the structures have many air leaks, but recently the airtightness and insulation of recent houses have been improved using insulation materials and films as shown in Figure1. However, many infiltration routes lurk in the spaces concealed inside the walls, the ceilings and the floors. In

Figure 1. Common wooden structure of Japanese house under construction

INTECH
open science | open minds

the concealed spaces, the pollutant sources for example, poly wood and glass wool are used. The crawl spaces are open to outside and insecticides are used to prevent termites and corrosion fungus in the spaces in most cases.

In order to prevent indoor air pollution, it is necessary to control emission rates of volatile organic compounds (VOC) from interior materials and to design effective ventilation routes. The prevention of infiltration of VOC from the concealed pollution sources is also needed as shown in Figure2. The authors made it clear that the concealed pollution sources influence indoor air quality and that the indoor concentrations increase rapidly when the exhaust ventilation system is used. To estimate the influence of the concealed pollution sources upon the indoor air quality, the ratios of the infiltration rates to the emission rates in the concealed spaces were used as an indicator. In a previous study reported in 2008, the ratios were measured in twelve detached houses in Japan and the status of the ratio was investigated using the measurement results and the results on the three test houses which had already been reported in 2005.

In this study, in order to find an effective method to reduce infiltration from the concealed spaces, the characteristics of the movement of chemical compounds in the concealed spaces and indoor spaces were investigated using building cut models and a simulation program named Fresh2006.
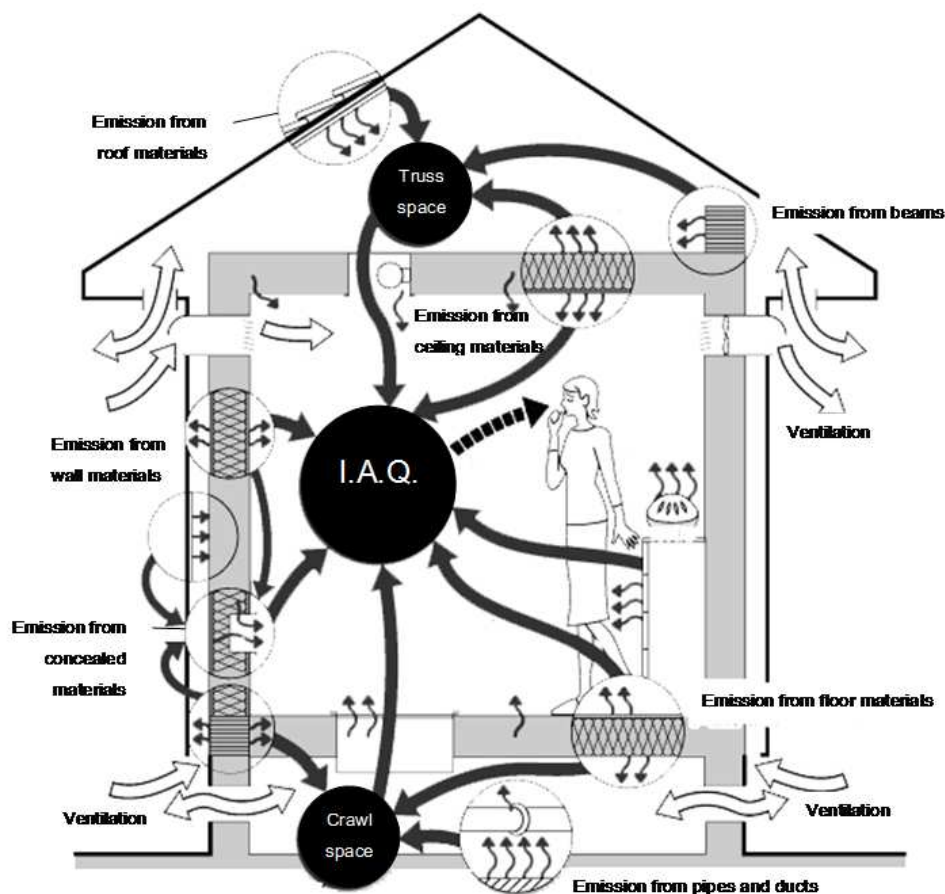
Figure 2. Infiltration of pollutants from the concealed spaces

Figure 3. Cut models of improved wooden post-and-beam structures and wooden stud structures

2. Measurement methods of infiltration ratio from concealed spaces

A ratio of the infiltration rate to the emission rate in the concealed space was used as an indicator. The ratios were calculated from the measurement results using two tracer gases. The influence of the concealed pollutant sources is explained basically using the following equations. The concentration in the indoor space C is given using equation 1 considering the infiltration from the concealed space to indoor space.

$$C = Et / Q + Co \qquad (1)$$

Where Et is the total emission rate of pollutants considering the infiltration from the concealed spaces, Co: the ambient concentration and Q ventilation rate.

Et is given as the next equation using κ: the infiltration ratio of pollutants from concealed spaces to indoor spaces.

$$Et = \kappa \, Ej + Ei \qquad (2)$$

Where Ej is the emission rate of pollutants in concealed spaces and Ei is the emission rate of pollutants in indoor spaces.

$$\kappa = \{(C-Co)\, Q - Ei\} \,/\, Ej \tag{3}$$

Two kinds of tracer gas were generated: one in the concealed space and the other in the indoor space. The concentrations were measured in the indoor space and the infiltration ratio was calculated using equation 3. At first, the ventilation rate Q was calculated using the generation rate and the concentration of the gas generated in indoor space. The infiltration ratio was calculated using the value of the ventilation rate Q and the data from another gas.

The ventilation rates, the infiltration ratios, the equivalent leakage areas per its floor areas, the air flow rate at the inlet or the outlet and the indoor and outdoor temperature and humidity were measured. The ventilation rates and the infiltration ratios were measured using two gases: sulphur hexafluoride (SF6) and freon22 (R22). A tracer gas was injected in the indoor space continuously. And the other tracer gas was injected to each concealed space as shown in Figure 5.

Figure 6 shows the change of tracer gas concentrations. When the concentrations became steady, the ventilation rates and the infiltration ratios were calculated using the stable concentrations and the injection rates were measured using mass flow controllers. These measurements were carried out without heating rooms to decrease the influence of temperature difference between indoor and outdoor upon the ventilation. The temperature differences were lower than ten degrees.
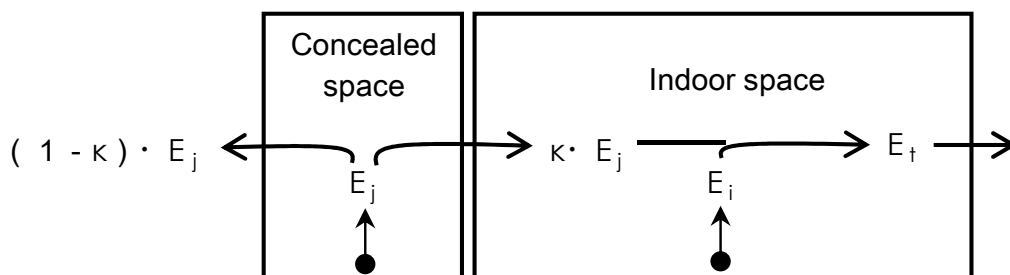

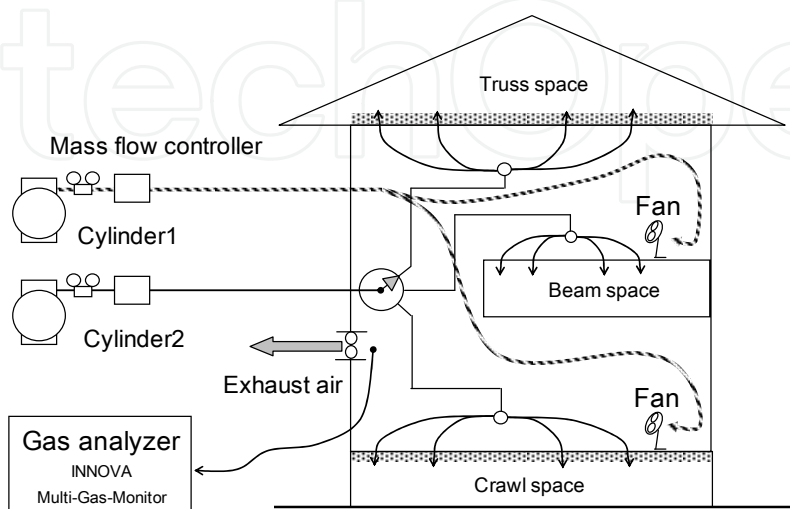**Figure 4.** Influence of the concealed pollutant source

Figure 5. System to measure the ventilation rates and the infiltration ratios
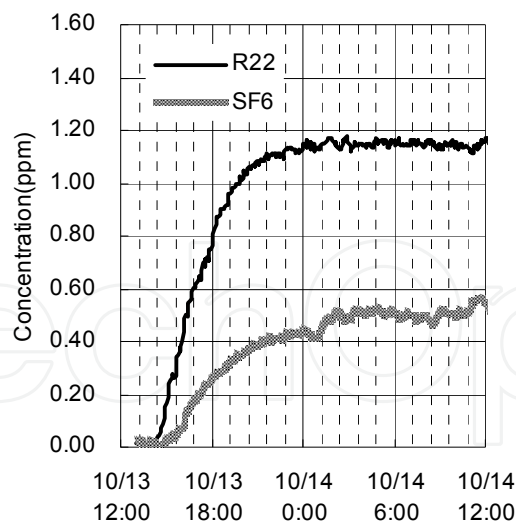
Figure 6. Change of concentrations of tracer gases

3. Simulation methods of the influence of infiltration upon I.A.Q.

The equivalent leakage areas in the concealed spaces were measured using cut models of wooden structures: a common post-and-beam wooden structure, an improved post-and-beam wooden structure built according to the latest building insulation code and a wooden (2 inch x 4 inch) stud structure built according to the latest building insulation code, which was established in 1999.

It was difficult to measure the equivalent leakage areas in the concealed spaces of real houses, so the cut models of these structures were constructed in a laboratory in Miyagigakuin Women's University. Figure 3 shows a cut model of improved post-and-beam wooden structure. The sizes of the elements of the cut model are the same as those of the elements of real houses but the height of the cut model was lower than a real house. The same size of cut model of improved post-and-beam wooden structure as a real house was built according to the latest insulation code was as the same size. These cut models include several leakages in the concealed spaces in these cut models. Cut models of a wooden (2 inch x 4 inch) stud structures were made in another method. Figure 3 shows divided cut models of wooden (2 inch x 4 inch) stud structures. Some partial cut models were made in order to save the space for measurement. These cut models were built by carpenters in the laboratory.

Leakage areas in the concealed spaces and the leakage areas between the concealed spaces and indoor spaces were measured using mass-flow controllers and pressure analyzers. Figure 7 shows the measurement system. When the leakage areas between cell1 and cell2 are measured, cell1 is controlled to be open to the outside and the air pressures of cell3 and cell4 are kept to be the same pressure as cell2. On this condition the air of cell2 goes only to cell1. The airflow rate from cell2 to cell1 accords the air flow rate through the mass-flow controller between the air tank and cell2, so the air flow rate can be known. Figure 8, Figure 9 and Figure 10 show the equivalent leakage areas per 1m of each structure.
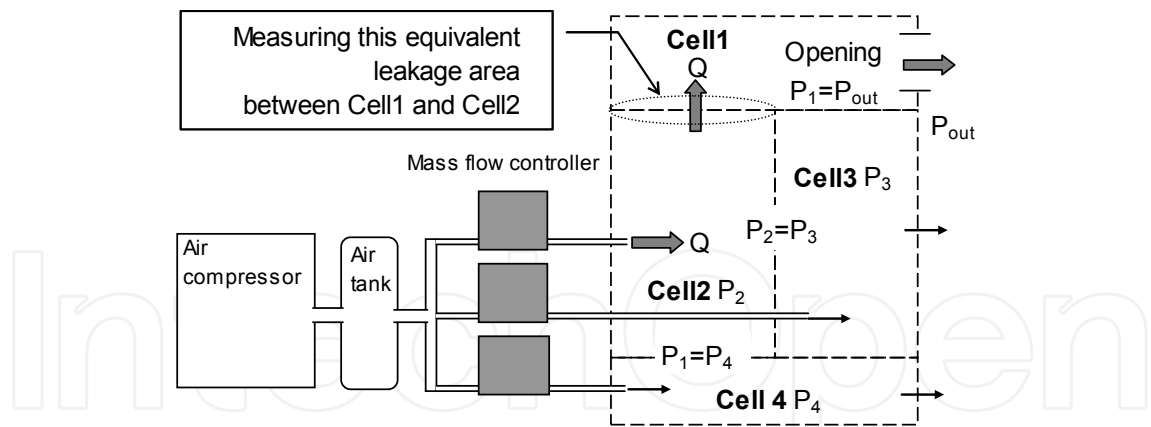
Figure 7. Measurement systems to measure leakage areas between cells
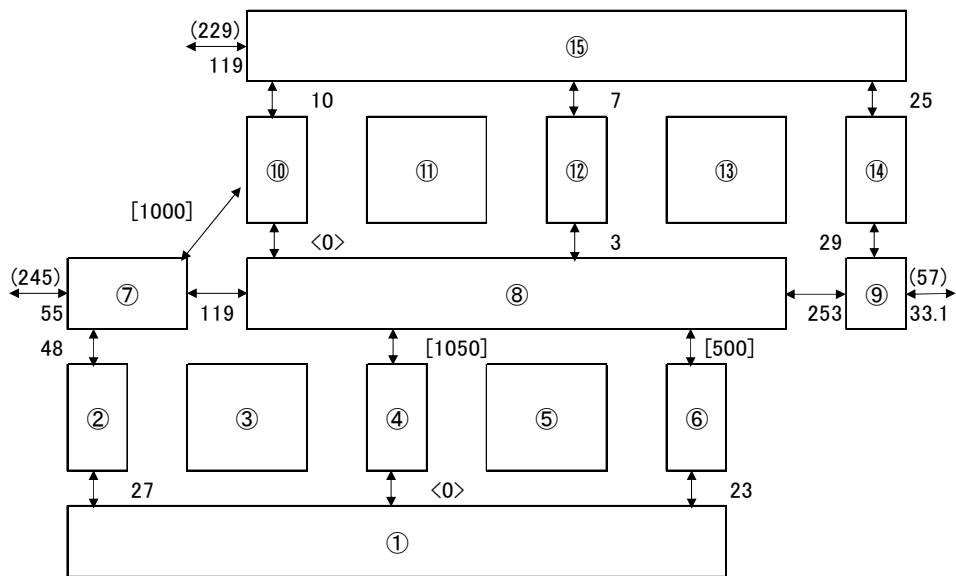

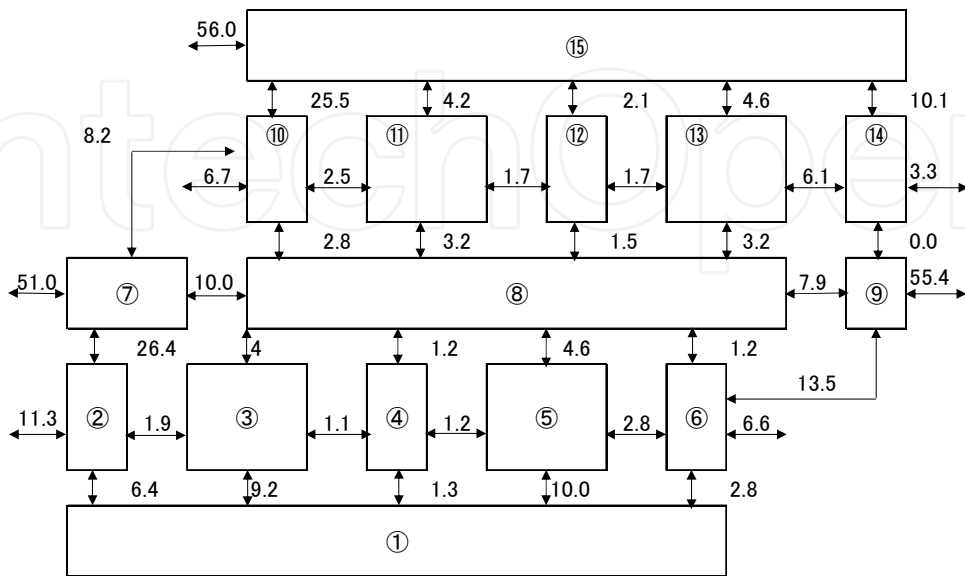**Figure 8.** Leakage network of a common post-and-beam structure (cm²/m)

Figure 9. Leakage network of an improved post-and-beam structure (cm²/m)
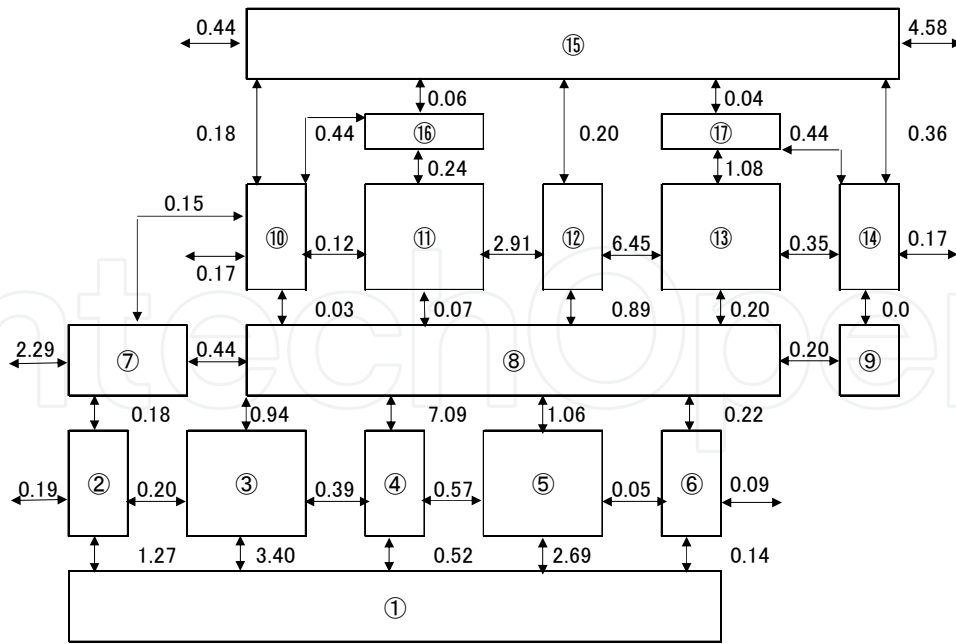
Figure 10. Leakage network of a wooden (2 inch x 4 inch) stud structure (cm²/m)

The movements of chemical compounds were calculated using a simulation program as in [4]. The program simulates the temperatures, the air flow rates, the concentrations and the generation rates of pollutants like formaldehyde, and carbon dioxide using the Japanese standard living schedule model by NHK as in [5] and the HASP weather data on Tokyo.

The simulation program was written in 1996, and was named 'Fresh96'. It was composed of the following three calculation methods.

1. Dynamic thermal calculation of temperature, heating and cooling loads: the calculation method was devised by Prof. Aratani, Hokkaido University in 1974. The initial responses of the thermal-flow rates are calculated and the functions of the responses are described as the following equation in order to increase the speed of the calculation.

$$h(t) = B_0 + \Sigma B_m e^{-\beta m \cdot t} + q \cdot \delta(t) \tag{4}$$

Where, $h(t)$ the initial response of thermal-flow rate, B_0 the steady value of thermal flow rate, $q = \Sigma B_m / \beta_m$ and $\delta(t)$ Delta function.

The temperatures and the heating and cooling loads are calculated with the above equation using Duhamel's integration method. Temperatures and heat loads are calculated using the calculated temperatures in other rooms and the calculated ventilation rates as values Δt before. In the following case studies, the interval time Δt was decided to be 5 minutes. The values are calculated using the standard weather data from Society of Heating, Air-conditioning and Sanitary Engineers of Japan and the rates of solar radiation through windows are calculated considering the effect of shades. The thermal loads by human behaviors such as cooking, watching television and cleaning rooms, are calculated from the daily schedule model of a family. The air-conditioners and the windows are operated to make the indoor climate comfortable considering the daily schedule of a family.

Calculation of air flow rate in the multi-cell system using the equation of power at the openings: the airflow rates are calculated using the following equations which are led by the balances of power at openings.

$$[D]\cdot\{q^n\}+[K]\{\int qdt\} = \{F_{wind}\}+\{F_{temp}\}+\{F_{fan}\} \tag{5}$$

where q the airflow rate, n the exponent of airflow friction, $[D]$ the matrix of airflow friction, $[K]$ the matrix of room air elasticity, $\{F_{wind}\}$ the power of wind, $\{F_{temp}\}$ the power by room air density $\{F_{fan}\}$ the power of fan.

The equations can be solved using Newmark's numerical integration method. The ventilation rates are calculated considering stack effect, wind pressure and mechanical power using the standard weather data, the ratios of wind pressure, the ratio of wind speed considering the circumstances and the performance of fans. In the case of the following studies, the ratio of wind speed at the town to the speed at the plain flat ground was 0.4.

Dynamic calculation of concentrations of pollutants using the equation of the amount of pollutants: the concentrations of pollutants in each room are calculated using the following equation which is led by the balance of the volume of pollutants.

$$[Q]\cdot\{C(t)\}+[V]\cdot\{C'(t)\}=\{M(t)\} \tag{6}$$

where $[Q]$ the matrix of airflow rate $Q(i,j)$: the airflow rate from room-i to room-j, $Q(k,k)= -\Sigma_{k\diamond i}Q(k,i)$, $C(t)$ the concentration of a pollutant, $[V]$ the volume of rooms, $\{M\}$ the emission rates of a pollutant in each room.

The equations can be solved using Newmark's numerical integration method. The emission rates of CO_2 are calculated using the average Japanese daily schedule and the data on the emission rates caused by people's behavior in houses shown in Table1. The daily schedule of each family in a house is calculated considering the plan of the house using the results of the survey on the Japanese daily schedule by NHK. Figure 11 shows the calculated emission rates of CO_2 on a holiday and a weekday in the house model. The emission rates of CO_2 change with the behavior of the family and the emission rates are high in the bedrooms on the second floor at night and the emission rates are high in the living room on the first floor at daytime. This is a typical pattern of emission rate of CO_2 in a general Japanese detached house.
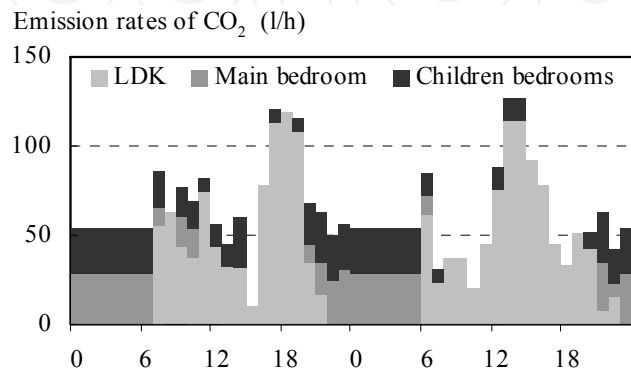

Figure 11. Calculated emission rates of CO2

The emission rates of formaldehyde were calculated using the following equation. The influences of temperature and sink were considered in the equation as in [6].

$$E = E25 \cdot a^{(T-25)} - \beta \cdot C(t) \tag{7}$$

Where E: emission rate (μg/h.m²), E_{25} (=100 μg/h.m²): emission rate measured in small chamber when temperature is 25deg.C, T: temperature, a=1.11: measured in small chamber, β (= 0.06): ratio of sink measured in small chamber, C(t): concentration (μg/m³)

In these studies, in order to make clear the influence of the infiltration of chemical compounds from beam spaces and a crawl space to indoor space upon the indoor air quality, SF6 was emitted at the beam spaces and R22 was emitted at the crawl space in the simulation models shown in Figure 12. Formaldehyde emission rates in the concealed spaces are set to be 100μg/h.m² considering the surface area of emission sources like plywood and the emission rates. This model was designed considering the shape of a low two-storied house. The emission rates of SF6 and R22 were 300 ml/h. The movements and the concentrations of each gas were calculated. The outdoor concentrations were set as follows. The concentration of carbon dioxide is 400 ppm, that of formaldehyde 0 μg /m³, that of SF6 0 ppm and that of R22 0ppm.
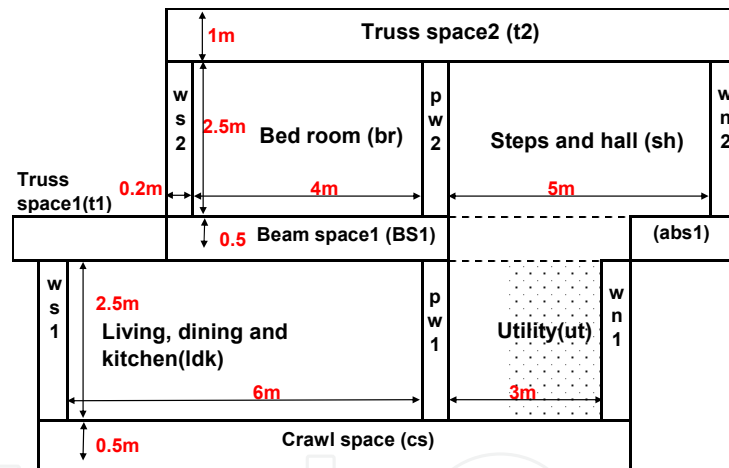

Figure 12. Building model for simulations

4. Adaptation of the measurement results of dwellers' behaviour on opening and closing windows

A monitor instrument to measure the open width at a sliding window was devised. The instrument consists of pulleys, a piece of string, a spring, a potential meter and a recorder as shown in Figure 13. When a dweller opens the sliding window, the sucking disk on the glass pulls the string and the pulley and the potential meter rotates. When a dweller closes the sliding window, the thread is rewound by the spring. The recorder records the resistance of the potential meter was recovered every 10 minutes. The open width was calculated using the recorded resistance. Not only the open width but the temperature and the humidity both in the room and outside were measured successively for almost a year in thirteen detached

houses from the temperate zone to the sub frigid zone in Japan. The living habits and the building types were investigated using a questionnaire form.

Figure14 shows the indoor temperature and the width of window opening. The width shows the president's behavior corresponding to weather condition. Figure 15 shows the change of the open width and the room temperature and the annual cycle of the relation between ambient temperature and open width.
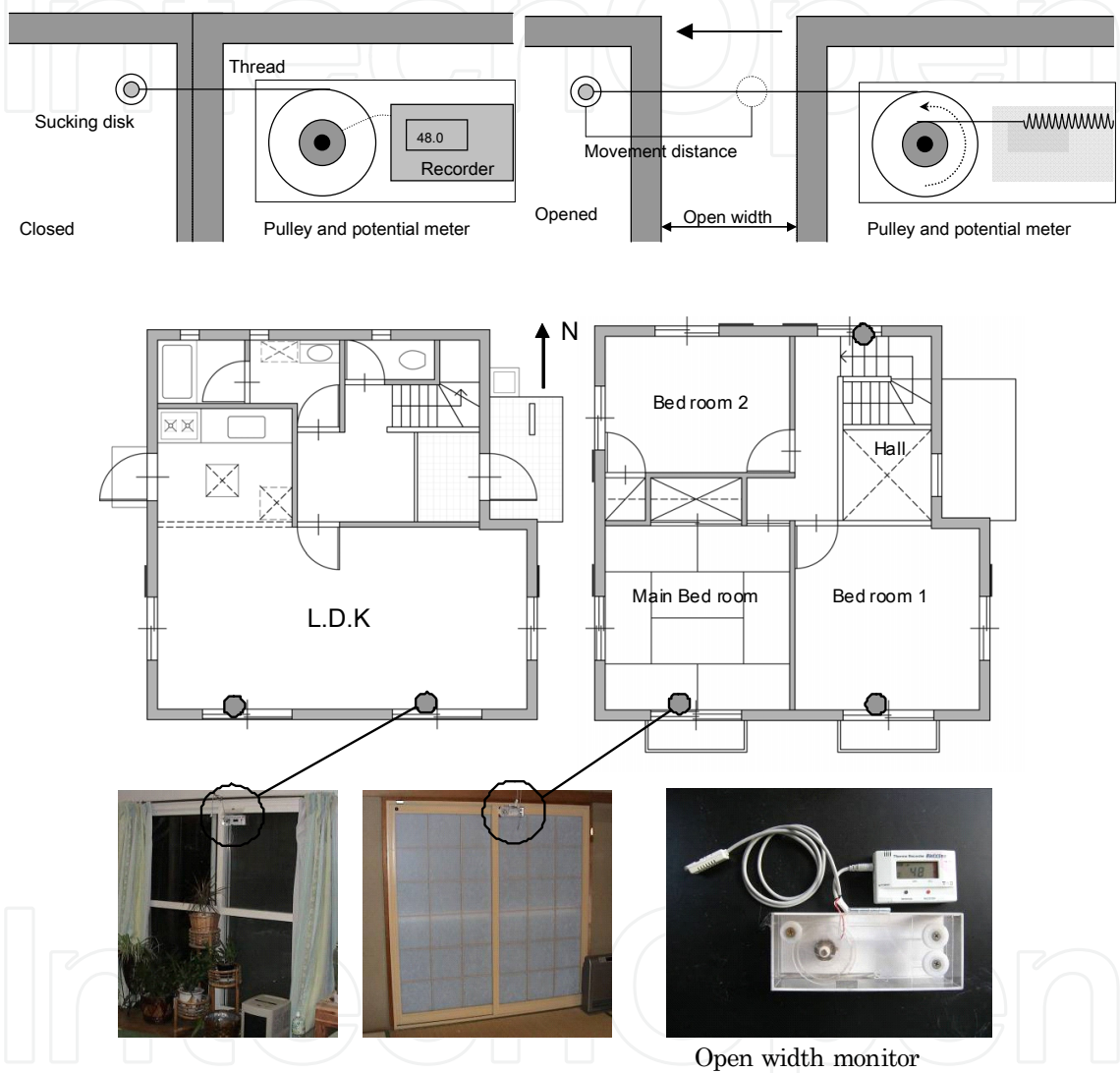

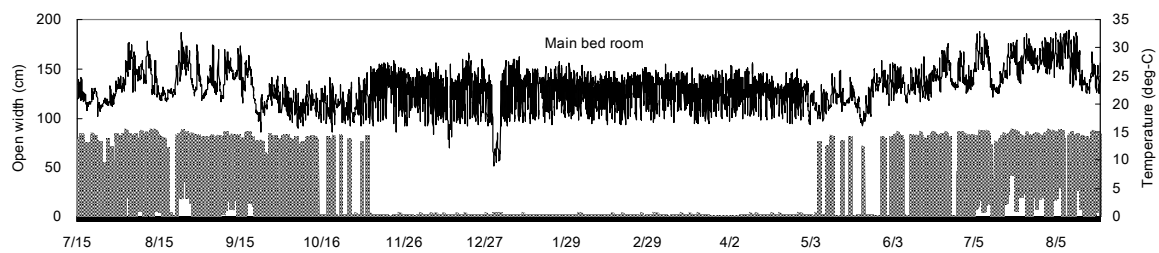**Figure 13.** Open width monitor at a sliding window

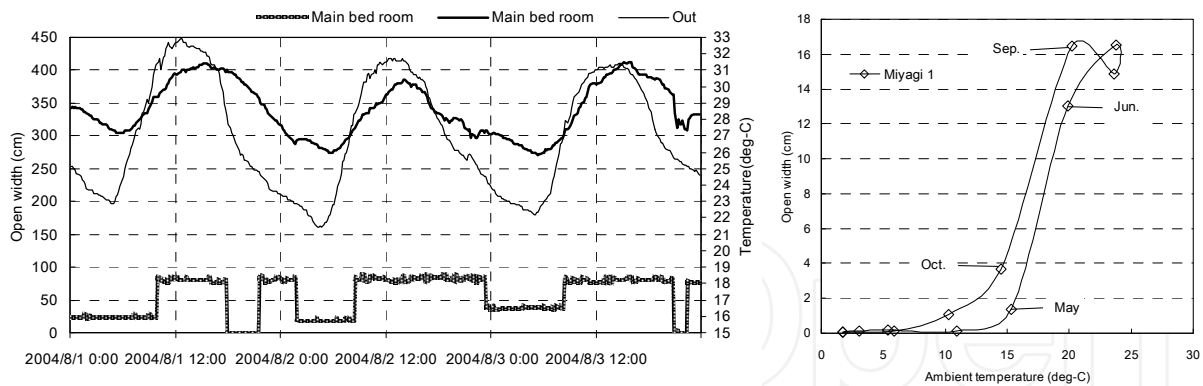**Figure 14.** Measured indoor temperature and open width in a bedroom

Figure 15. Open width and temperatures in a house

The results of the measurement showed that the averages of open widths were very small even in hot season and mild season. The open width was large when they open window, but windows were open for a very short in hot season. The results of questionnaire survey showed that the reasons: windows were closed were insects, noise and the prevention of criminals. The closing habit was detected clearly in the case of the measured open width in the room on the first floor.

The open width changes with the indoor temperature and the living style. When dwellers go into the room and feel hot, they open windows. In many cases, they close windows when they leave the room. Therefore the open width changes with the dweller's living schedule. The open width is influenced by the indoor and outside temperature. Dwellers keep open width a few centimeters to ten centimeters when they feel a little hot. Such small open widths were shown at night in many cases. When they feel very hot, they close windows and turn on the air conditioner.

The simulations were made on the following conditions based on the results mentioned above. The dwellers operate air-conditioner and windows when they use the room. When they are sleeping, they don't operate windows. The grades of open width were 1: closed (0cm), 2: slit open (10cm) and 3: full open (80cm). The indoor temperature is higher than 26 deg-C, the grade was made up and when the indoor temperature is lower, the grade was made down. If the temperature became higher than 28 deg-C, the grade was set to 1 and the room was cooled by air conditioner. If the temperature became lower than 22 deg-C, the room was heated by air conditioner. These operations were made at the interval of one hour. The simulation was made using HASP weather data of Tokyo.

5. Results of simulations

The equivalent leakage areas of the three structures were measured using this simulation program. A large fan was set and the inside air was exhausted. The airflow rates are controlled to meet five ranks of airflow rate and the pressure differences were calculated. The equivalent leakage areas were also calculated. The equivalent leakage area of the model with a common wooden structure was 5.0 cm^2/m^2, that of an improved structure was 2.8 cm^2/m^2 and that of a wooden (2 inch x 4 inch) stud structure was 0.3cm^2/m^2.

Figure 16 and Figure 17 show the hourly change of formaldehyde concentrations in winter. The concentrations in the beam space (bs1) in the case of exhaust and supply ventilation in Figure 17 is higher than those in the case of exhaust ventilation in Figure 16. The formaldehyde stays longer in the beam space in the case of an exhaust and supply ventilation. But the indoor concentrations are lower in the case of exhaust and supply ventilation. These results show that the influences of the concealed spaces upon the indoor air concentrations depend on the ventilation method.
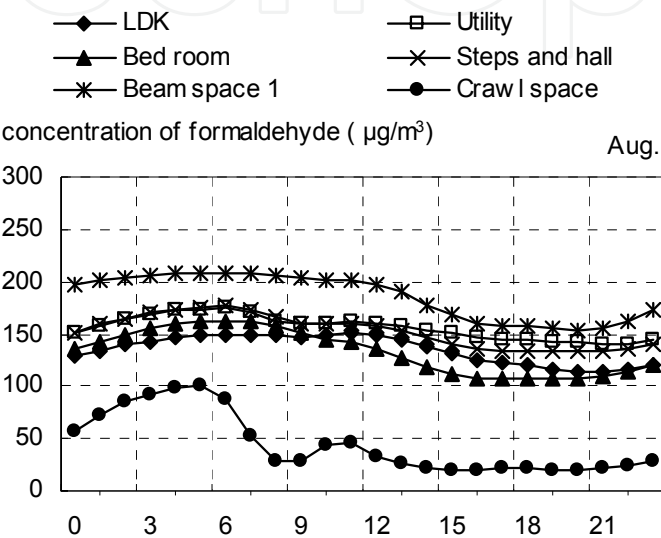
Figure 16. Hourly change of formaldehyde in a house with an improved structure and an exhaust ventilation system
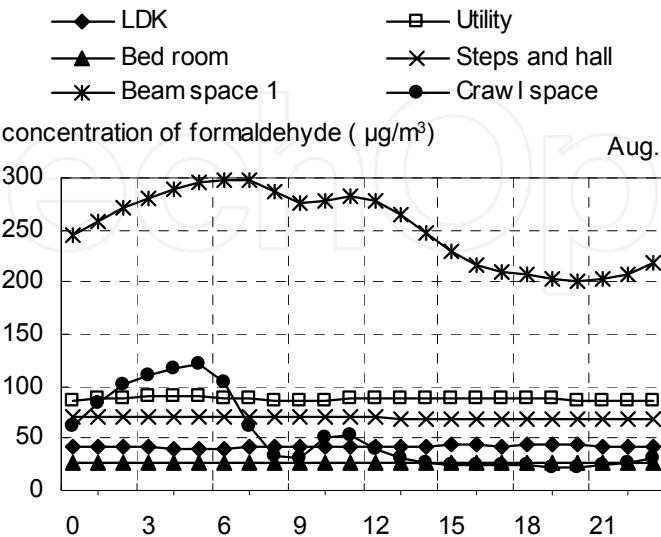

Figure 17. Hourly change of formaldehyde in a house with an improved structure and an exhaust-and-supply ventilation system

Figure 18 and figure 19 show the airflows in a common structure. In the case of exhaust ventilation in figure 18, the air goes from concealed spaces to indoor spaces. The air goes from the crawl space to the indoor space on the second floor through the wall and truss space (t1). Several routes from concealed spaces to indoor spaces are shown in these figures. In the case of exhaust and supply ventilation in Figure19, these routes are also recognized.
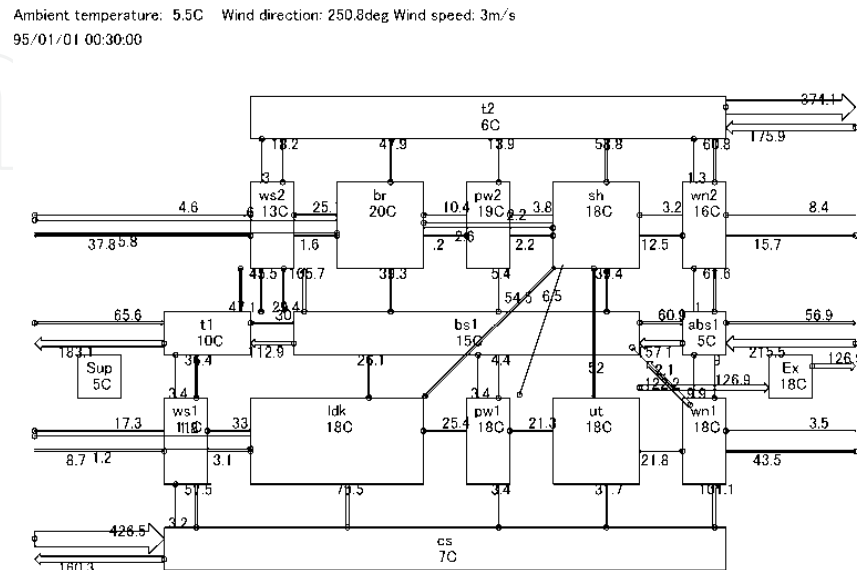

Figure 18. Calculated airflow rates in a common structure with an exhaust ventilation system
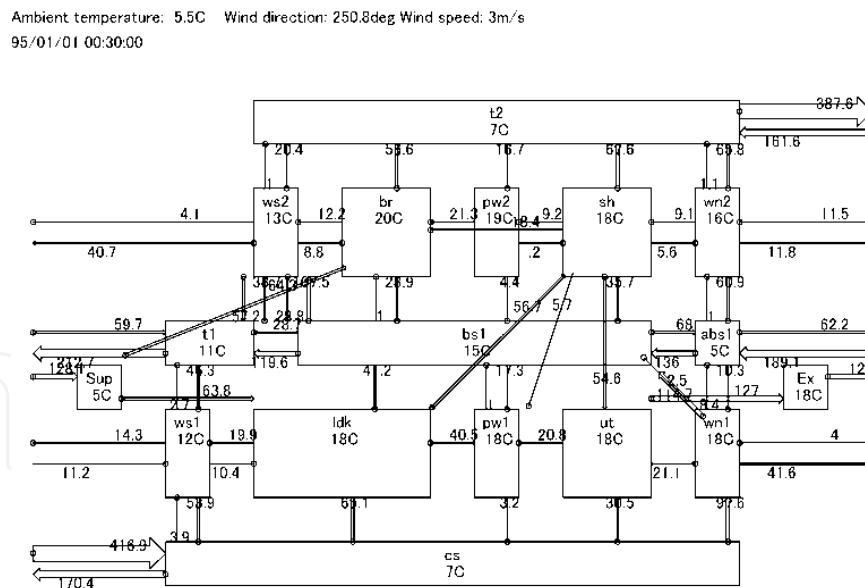

Figure 19. Calculated airflow rates in a common structure with an exhaust and supply ventilation system

Figure 20 and Figure 21 show the airflows in the case of exhaust ventilation. The airflow rates through the above routes became lower in these airtight structures: an improved structure and a wooden (2 inch x 4 inch) stud structure. The airflow rates through these routes become very low in the cases of airtight structures.
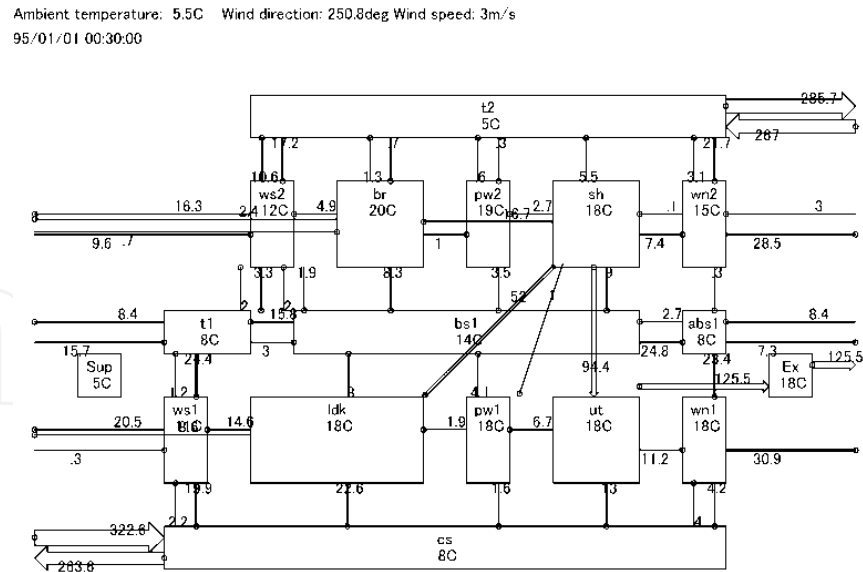
Ambient temperature: 5.5C   Wind direction: 250.8deg Wind speed: 3m/s
95/01/01 00:30:00

Figure 20. Calculated airflow rates in an improved structure with an exhaust ventilation system

Ambient temperature: 5.5C   Wind direction: 250.8deg Wind speed: 3m/s
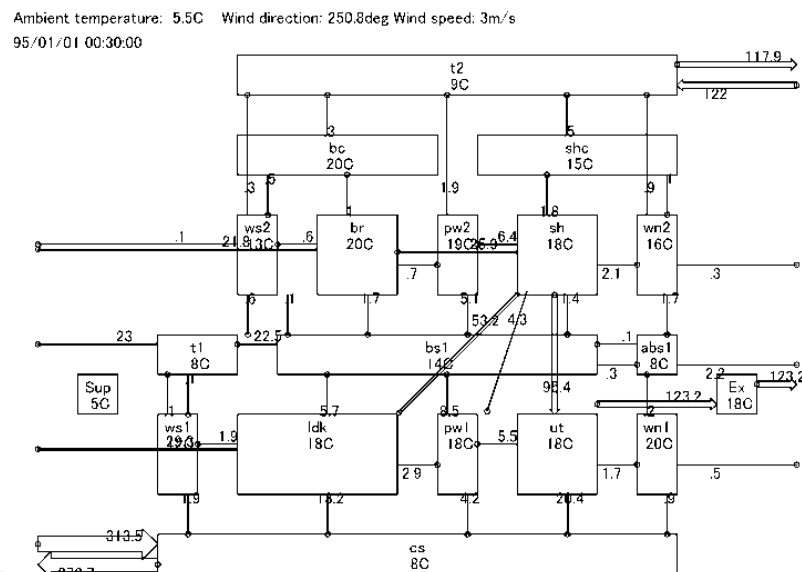95/01/01 00:30:00

Figure 21. Calculated airflow rates in a wooden (2 inch x 4 inch) structure with an exhaust ventilation system

Figure 22 shows the annual change of temperature difference and wind speed in Tokyo. Figure 23 shows the calculated airflow rates directly from the outside to indoor spaces. In mild seasons like June and September, some airflow rates became higher than in winter, because the windows were opened to make indoor climate comfortable. In mid-summer, the indoor spaces were cooled by air conditioner and these airflow rates became lower than those in mild seasons.

Figure 24 shows the annual change of calculated concentrations. These concentrations are monthly averages. The concentrations of carbon dioxide were steady and low. The
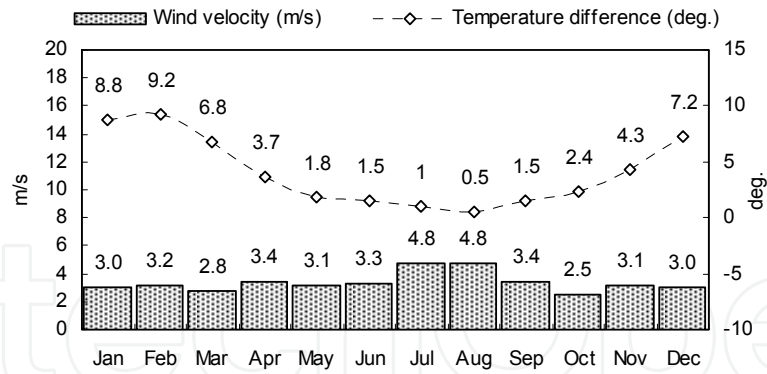
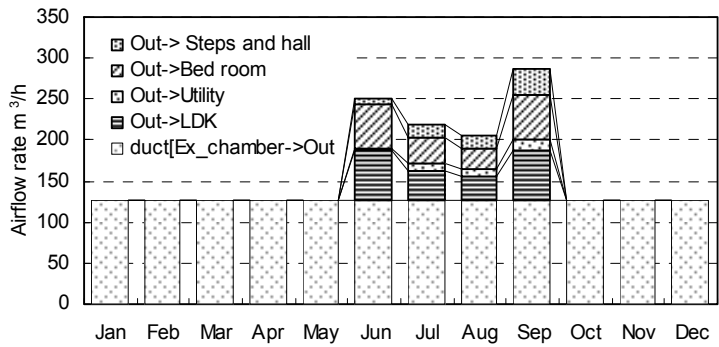**Figure 22.** Annual change of temperature difference and wind speed

Figure 23. Airflow rates in an improved structure with an exhaust and supply ventilation system
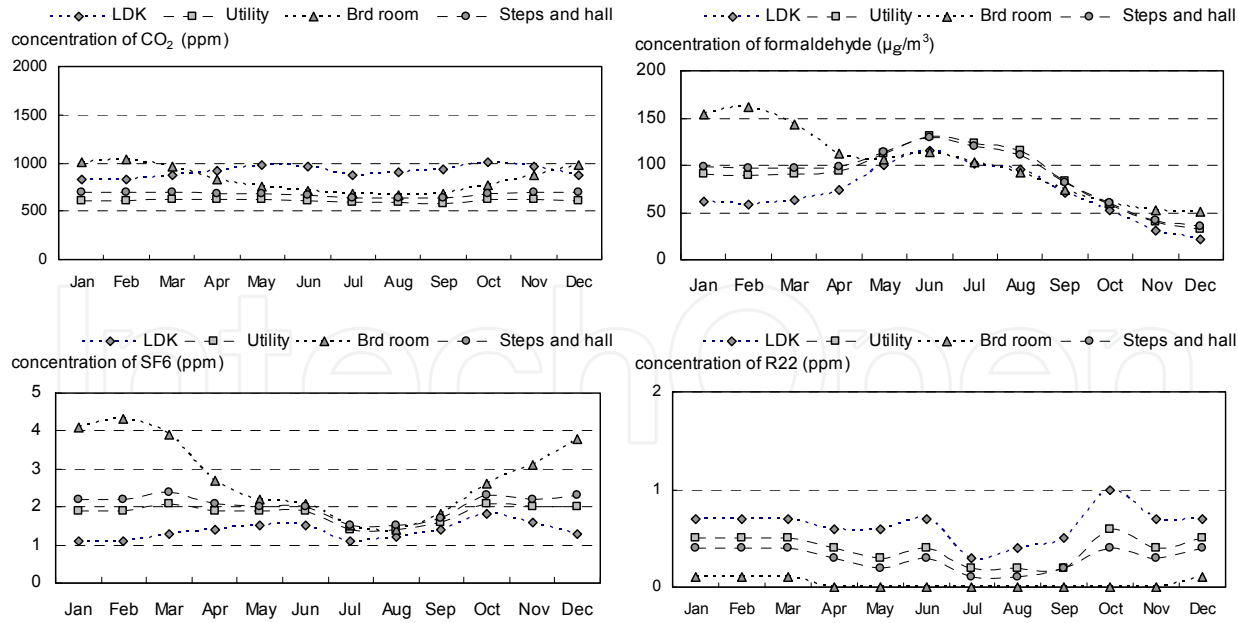

Figure 24. Calculated concentrations in an improved structure with an exhaust ventilation system

concentrations in the bedroom (br) were the highest because the air supply through the ventilator was not high enough. These characteristics were shown in common structures with many air leaks. The annual change of formaldehyde concentrations shows interesting

characteristics. Generally, the concentrations decrease but the concentrations were high in summer except for the concentrations in bedroom that were high in early months of the year. These characteristics were based on the following mechanisms. The emission rate of formaldehyde increases with temperature. The emission ability declines with the integral volume of emission.

SF6 is emitted in the beam space (bs1). The concentrations of SF6 are low in summer and the concentrations in the bedroom (br) are higher than those in other spaces. In winter, the air supply to bedroom is not high enough due to large temperature differences but it becomes sufficient in mild seasons and summer. In mild seasons windows were opened. These changes of conditions influenced the changes of concentrations.

R22 is emitted in the crawl spaces (cs). The concentrations of R22 are lower than SF6 concentrations. The crawl spaces are connected to the outside through openings according to the building code to keep wooden structures. But the indoor concentrations were not zero. This result shows that it is necessary to keep the emission rates of chemical compounds like organic phosphorus insecticide low even in the crawl space.
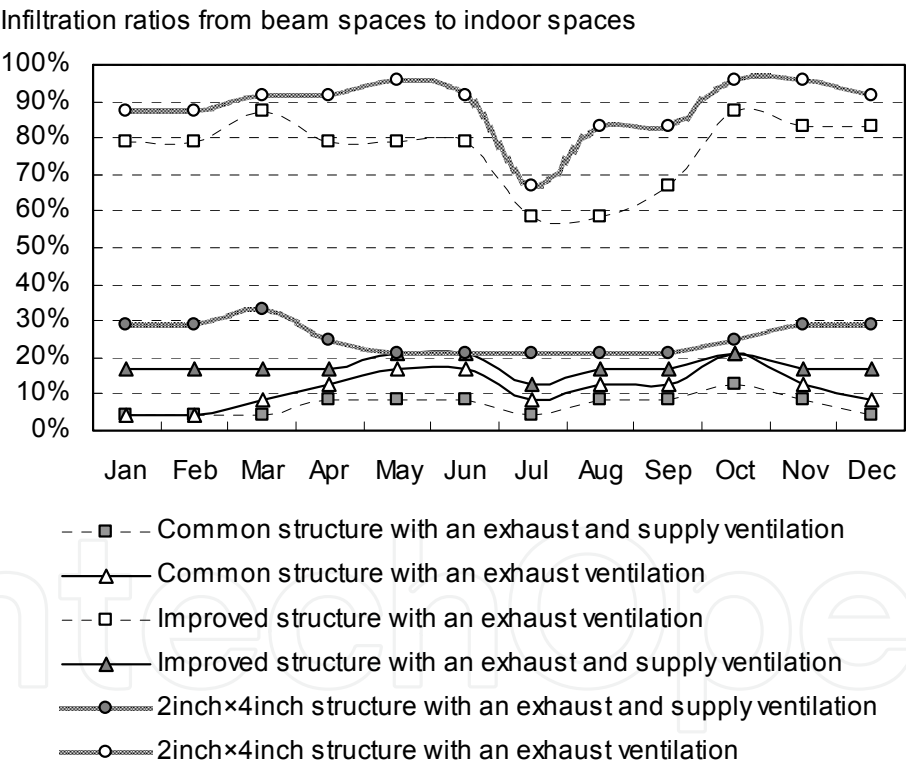
Infiltration ratios from beam spaces to indoor spaces

--■-- Common structure with an exhaust and supply ventilation

—△— Common structure with an exhaust ventilation

--□-- Improved structure with an exhaust ventilation

—△— Improved structure with an exhaust and supply ventilation

••••●•••• 2inch×4inch structure with an exhaust and supply ventilation

••••○•••• 2inch×4inch structure with an exhaust ventilation

Figure 25. Annual changes of infiltration ratios from the concealed spaces to indoor spaces

Figure 25 shows the infiltration ratios from beam space to indoor space. The infiltration ratio accords to a ratio: κ of the infiltration rate of gas to indoor spaces to the emission rate in concealed spaces. The ratios are high in the cases of exhaust ventilation system and airtight structures. In these cases, indoor spaces are decompressed and pollutants are pulled inside from the concealed spaces. Therefore when windows are open, the ratios become lower. In the case of crawl spaces, the ratios are lower than those in the case of beam space.

Figure 26 shows the comparison of concentrations. In the case of carbon dioxide, the concentrations are higher with an exhaust ventilation system and an airtight structure. This tendency is much stronger in the case of formaldehyde, SF6 and R22.

Figure 27 shows the infiltration ratios from concealed spaces to indoor spaces. The figure also shows the tendency mentioned above and shows that it is necessary to design ventilation routes considering air leaks and the emission of pollutants in the concealed spaces for better indoor air quality.
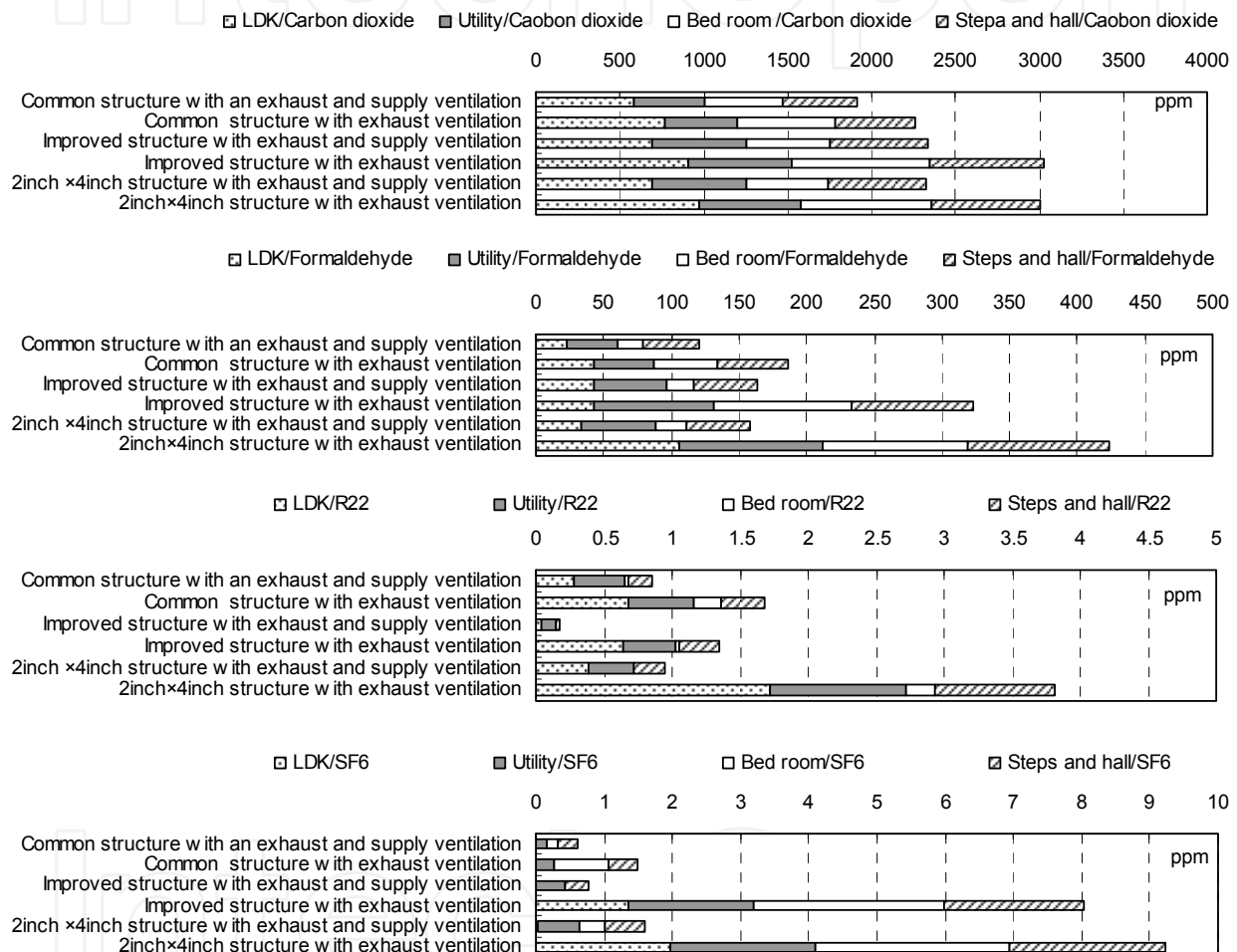

Figure 26. Calculated indoor concentrations of each case study
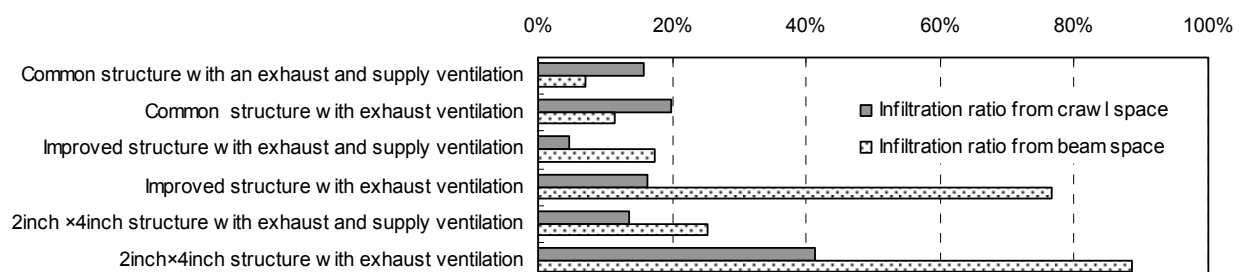

Figure 27. Infiltration ratios from the concealed spaces to indoor spaces in each case study

The calculated infiltration ratios were compared with the measured ratios in real houses: common wooden houses, prefabricated houses and a wooden (2 inch x 4 inch) stud houses as shown in Figure 28. The ratios are measured using tracer gases: SF6 and R22. The tracer gases are emitted constantly in the concealed spaces and in the indoor spaces and the concentrations were measured indoors. The ratios were calculated from the concentrations and the emission rates.

The calculated infiltration ratio from beam space increases with the decompression level. The calculated ratio in the case of a wooden (2 inch x 4 inch) stud structure is the highest and the level of decompression is also the highest. In the case of a common structure, the calculated ratio and the decompression level are both the lowest. The measured ratios have the same tendency. In the case of the ratio from crawl spaces, the measured ratios are lower but the above-mentioned tendency remains.
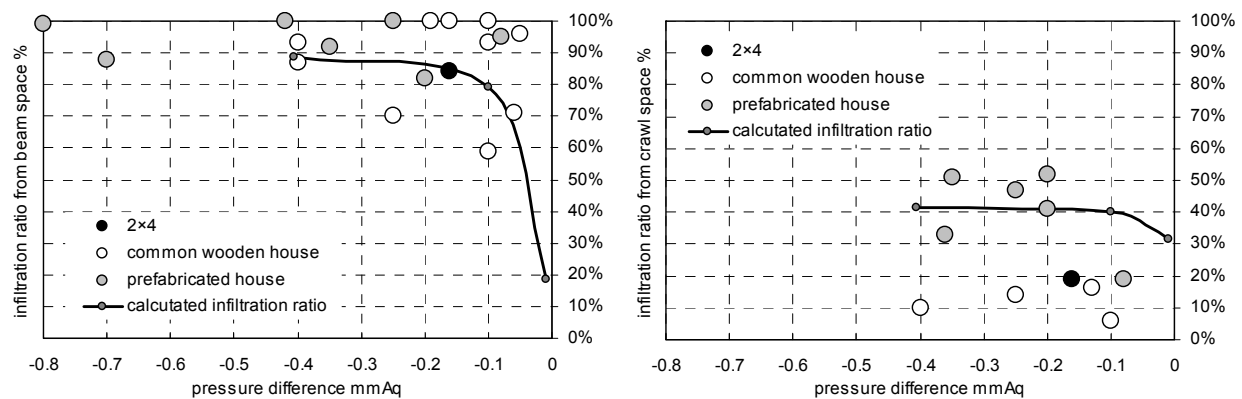

Figure 28. Comparison between the calculated infiltration ratios and the measured ratios in real houses

6. Conclusions

The concealed infiltration routes were shown by the measurements of equivalent leakage areas using cut models of Japanese houses and the simulation considering the weather and Japanese living habit. The indoor concentrations of the chemical compounds which volatilized in concealed spaces changed with the weather and the behaviors of the residents. The infiltration ratios from the concealed spaces to indoor spaces were influenced by mechanical ventilation. The influence of the infiltration upon the indoor air quality was larger in the house with an exhaust ventilation system than with any other ventilation system. These results show that it is necessary to consider the materials and the leakages in the concealed spaces for a countermeasure against sick house syndrome especially in the case of exhaust ventilation. The results will show a guide line for designing a house with better indoor air quality.

Nomenclature

B_0: the steady value of thermal-flow rate
$C(t)$: the concentration of a pollutant

[D]: the matrix of airflow friction

{F$_{temp}$}: the power by the room air density

{F$_{wind}$}: the power of wind

h(t): the initial response of thermal-flow rate

[K]: the matrix of room air elasticity

{M}: the emission rate of a pollutant in each room.

n: the exponent of airflow friction

q : the airflow rate

 [Q]: the matrix of airflow rate

Q(i,j): the airflow rate from room-i to room-j

[V]: the volume of a room

δ(t): Delta function

Author details

Motoya Hayashi
Miyagigakuin Women's University,Japan

Yishinori Honma
Iwate Prefectural University, Japan

Haruki Osawa
National Institute of Public Health, Japan

Acknowledgement

7. References

[1] Motoya Hayashi, Haruki Osawa: The influence of the concealed pollution sources upon the indoor air quality in houses, The International Journal of Building Science and its Applications，BUILDING AND ENVIRONMENT,Vol.43,pp.329-336,2008

[2] Hiroshi Yoshino, Kentaro Amano, Mari Matsumoto, Koji Netsu, Koichi Ikeda, Atsuo Nozaki, Kazuhiko Kakuta, Sachiko Hojo and Satoshi Ishikawa, 2004. Long-Termed Field Survey of Indoor Air Quality and Health Hazards in Sick House, Journal of Asian Architecture and Building Engineering, Vol. 3 (2004) No. 2 pp.297-303

[3] Haruki Osawa, Motoya Hayashi: Status of the indoor air chemical pollution in Japanese houses based on the nationwide field survey from 2000 to 2005, The International Journal of Building Science and its Applications BUILDING AND ENVIRONMENT, Vol.44, pp. 1330-1336, 2009

[4] M.Hayashi, M.Enai and Y.Hirokawa, 2001. "Annual characteristics of ventilation and indoor air quality in detached houses using a simulation method with Japanese daily schedule model", The International Journal of Building Science and its Applications 'BUILDING AND ENVIRONMENT' Vol.36, No.6 July 2001,721-731

[5] NHK. 1990. "The survey on the Japanese daily schedule 1990"

[6] Rika Funaki and Shin-ichi Tanabe, 2002. Chemical Emission Rates from Building Materials Measured by a Small Chamber, Journal of Asian Architecture and Building Engineering, Vol. 1 (2002) No. 2 pp.2_93-100